3D Tensor Normalization for Improved Accuracy in DTI Tensor Registration Methods

Aditya Gupta[1], Maria Escolar[1], Cheryl Dietrich[2], John Gilmore[2], Guido Gerig[3], Martin Styner[2][4]

[1] Department of Pediatrics, University of Pittsburgh
[2] Department of Psychiatry, University of North Carolina at Chapel Hill
[3] Scientific Computing and Imaging Institute, University of Utah
[4] Department of Computer Science, University of North Carolina at Chapel Hill

Abstract. This paper presents a method for normalization of diffusion tensor images (DTI) to a fixed DTI template, a pre-processing step to improve the performance of full tensor based registration methods. The proposed method maps the individual tensors of the subject image in to the template space based on matching the cumulative distribution function and the fractional anisotrophy values. The method aims to determine a more accurate deformation field from any full tensor registration method by applying the registration algorithm on the normalized DTI rather than the original DTI. The deformation field applied to the original tensor images are compared to the deformed image without normalization for 11 different cases of mapping seven subjects (neonate through 2 years) to two different atlases. The method shows an improvement in DTI registration based on comparing the normalized fractional anisotropy values of major fiber tracts in the brain.

Keywords: Tensor Normalization, DTI Registration, DTITK.

1 Introduction

Diffusion tensor imaging (DTI) is a magnetic resonance imaging (MRI) technique that enables the measurement of restricted diffusion of water molecules in tissue to produce neural tract images. This technique has become increasingly important for studies of anatomical and functional connectivity of the brain regions. DTI is now extensively used to study the fiber architecture in the living human brain via DTI tractography. This technique has proven especially valuable in clinical studies of white matter (WM) integrity in the developing brain for diseases, such as metachromatic leukodystrophy (MLD), cerebral palsy and Krabbe. In this paper, the tensor normalization method is tested on a particular white matter demyelinating disease called Krabbe [1].

Krabbe disease (also called globoid cell leukodystrophy) is a rare, often fatal genetic disorder of the nervous system caused by a deficiency of an enzyme called galactocerebrosidase, which aids in the breakdown and removal of galactolipids found in myelin. Previous studies show that patients with infantile Krabbe disease have lower fractional anisotropy (FA) across the corpus callosum and along

the DTI fiber bundle of internal capsules (IC) when compared with healthy age-matched controls [1]. Based on the above findings, atlas based fiber tract analysis is used for analyzing DTI of Krabbe subjects [2]. There are considerable anatomical variations between the Krabbe subjects and the atlas and hence for accurate analysis of white matter fiber tracts it is crucial to establish a registration based voxel-wise correspondence between a normal control neonate DTI atlas and the Krabbe subjects. To achieve this needed registration accuracy, the research presented in this paper provides a method to improve the state-of-the-art approach to individually register DTI images into the atlas space.

The registration of diffusion tensor images is particularly challenging when compared to registering scalar images as DTI data is multi-dimensional and the tensor orientations after image transformations must remain consistent with the anatomy. Prior to the development of full tensor based registration methods, DTI registration was performed with traditional image registration algorithms on scalar images derived from the DTI[3]. These methods discard the orientation component of the data and thus DTI registration algorithms that directly use higher order information of DTIs, such as the corresponding principal eigenvectors [4] and the full tensor information [5] are now preferred. In our recent publication [6], the performance of scalar and full tensor registration algorithms are compared for Krabbe neonates. In comparison to the commonly available regsitration packages, the full tensor based DTI-TK [5] method showed the most accurate registration performance. DTI-TK is a non-parametric, diffeomorphic deformable image registration that incrementally estimates its displacement field using a tensor-based registration formulation. It is designed to take advantage of similarity measures comparing whole tensors via explicit optimization of tensor reorientation. Hence, in this paper the method is tested with the DTI-TK registration tool.

Normalization of DTIs is challenging as the data is multidimensional and includes considering the shape of the tensors along with tensor properties such as FA. Methods to improve DTI registration have been proposed by determining the correspondence between tensors using Gabor filters [7]. For normalization, the full tensor registration methods like DTI-TK [5] uses the ADC profile information. The F-TIMER [4] method uses the local statistical information of underlying fiber orientations along with the edge strength of the FA and the ADC maps for normalization. In both methods, the normalization is specific to the methods developed and may not always result in good normalization if there are considerable differences in local tensor appearance between the case and the template, for example, in the mapping of a neonate to a 2 year template. In this paper, our aim is to develop a general tensor normalization step that can be incorporated in the analysis pipeline as a prior step to any full tensor based registration algorithms.

For DTI derived scalar image registration methods, a simple histogram normalization of the subject to the template improves the performance of registration considerably [8]. Motivated by these approaches, this paper presents a normalization method for full tensor registration methods that normalizes the 3

dimensional Eigenvalues of each tensor while maintaining similar FA values. The deformation fields are computed using the full tensor registration methods on the normalized DTI images, and the fields are applied on the original DTIs. The performance with and without normalization are compared based on normalized FA values of major fiber tracts of the brain.

2 Method

For scalar image registrations based on sum of squared differences, histogram based intensity normalization is commonly used prior to registration to improve the registration accuracy. Similarly for DTI derived scalar images such as FA images, histogram based intensity normalization is used to determine an improved deformation field. This normalization is achieved by computing the histograms of the subject I_{sub} and the template I_{temp} scalar image. From the histograms, the cumulative distribution functions (cdfs) of the two images C_{sub} and C_{temp} are determined. For each image intensity n_i, an intensity level n_o, for which $C_{sub}(n_i) = C_{temp}(n_o)$ is computed; this is the result of histogram matching function $M(n_i) = n_o$. The histogram matching function applied on each voxel of the subject image gives the normalized FA images. In this paper, we extend this idea of scalar intensity normalization 3D tensors in DTI.

Diffusion tensor MRI characterizes the diffusion of water molecules by measuring the apparent diffusion tensor in each voxel of an MRI volume. The method assumes that water molecules move according to a simple anisotropic diffusion process so that the displacement x of a water molecule over a fixed time t is modeled as a random variable that follows the multivariate normal distribution p with the mean at the origin and covariance $2tD$, where D is the diffusion tensor, a symmetric and positive-definite 3-by-3 matrix. The Eigenvalues $\lambda_1, \lambda_2, \lambda_3$ of D are used to determine the standard DTI properties like mean diffusivity (MD) and FA defined by:

$$MD = (\lambda_1 + \lambda_2 + \lambda_3)/3; FA = \sqrt{\frac{(\lambda_1 - \lambda_2)^2 + (\lambda_2 - \lambda_3)^2 + (\lambda_1 - \lambda_3)^2}{\lambda_1^2 + \lambda_2^2 + \lambda_3^2}} \quad (1)$$

Our proposed method, works in this three dimensional Eigenvalue space by first determining the cdf planes. The standard cdf equation for three values $\lambda_1, \lambda_2, \lambda_3$ is defined by the equation:

$$C_{in}(\lambda_{1a}, \lambda_{2a}, \lambda_{3a}) = p((0 \leq \lambda_1 \leq \lambda_{1a}), (0 \leq \lambda_2 \leq \lambda_{2a}), (0 \leq \lambda_3 \leq \lambda_{3a})) \quad (2)$$

In the 3D space, the summation cdf volume based on this equation is a rectangular box. Our aim in this paper is to nomalize two DTI volumes while maintaining a similar cumulative distribution function and also to maintain a similar distribution of mean diffusivity. To achieve this aim, we propose to modify this equation to have constant cdf planes rather than constant cdf rectangular volumes. The modified 3-D cdf equation is defined as:

$$C_{in}(\lambda_{1in}, \lambda_{2in}, \lambda_{3in}) = p((\lambda_1 + \lambda_2 + \lambda_3 \leq 3MD_i)) \quad (3)$$
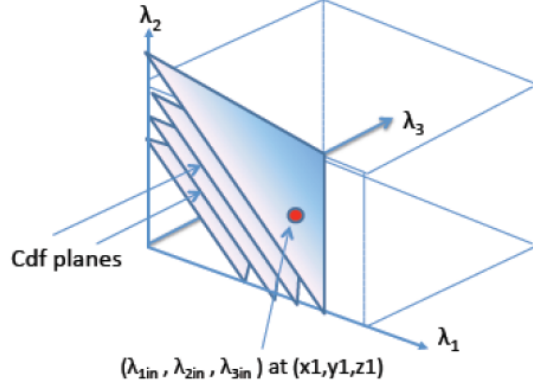
4

Fig. 1. Constant cdf planes - iso-MD planes defined in the subject and atlas eigen value space.

where $MD_i = (\lambda_{1in} + \lambda_{2in} + \lambda_{3in})/3$. The summation volume is bound by a plane which has the same cdf values as shown in Fig. 2. The input cdf is a function of MD. Since these planes have constant MD values for all points $(\lambda_1, \lambda_2, \lambda_3)$ lying on the plane, in further discussion we refer to these constant cdf planes as iso-MD planes. Ji-Hee et. al. [9] presents a similar argument and result for color normalization in the r, g, b space.

The proposed method is discussed below step-by-step and is shown in Fig. 3. Based on the above proposed idea of constant cdf planes, the first step of the algorithm is to define iso-MD planes in the subject and the atlas eigen value space with fixed intervals $'\delta'$, a concept similar to defining histogram bins. The value of $'\delta'$ is selected based on the Eigenvalues of tensors of the subject and the atlas. The following steps are repeated for each tensor of the subject. Each subject tensor (for discussion consider tensor at particular location (x, y, z)) is mapped to the closest iso-MD plane. The atlas iso-MD plane with the closest cdf value to the selected subject iso-MD plane is determined based on the equation $C_{out}(MD_{out}) = C_{in}(\lambda_{1x1,y1,z1}, \lambda_{2x1,y1,z1}, \lambda_{3x1,y1,z1})$. This equation ensures a uniform cumulative distribution function between the normalized subject tensors and the atlas tensors. In fact, any selection of positive $\lambda_1, \lambda_2, \lambda_3$ value lying on this atlas iso-MD plane will lead to a uniform cdf. Let us refer to the set of points on the atlas iso-MD plane $'i'$ as $\lambda_{1i,MD}, \lambda_{2i,MD}, \lambda_{3i,MD}$, the subscript 'MD' indicating that all the points on this plane have constant MD. The next step is to find the particular $\lambda_1, \lambda_2, \lambda_3$ value on the iso-MD plane that best normalizes the subject case to the atlas space. For this, we need to determine the atlas normalized FA value for the tensor. This is achieved by applying a standard 2D histogram matching of the subject FA scalar image to the atlas FA scalar image as discussed below.
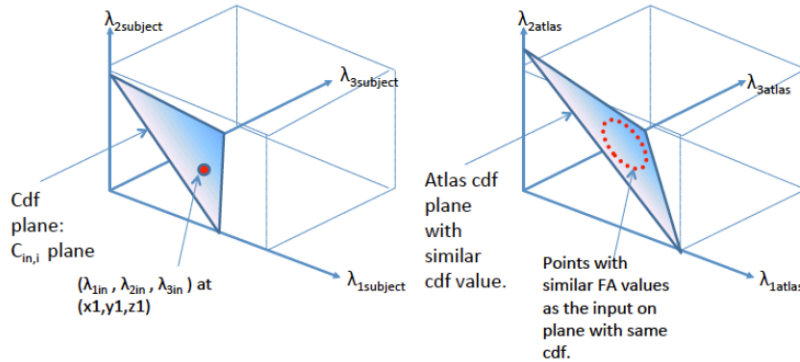
Fig. 2. Mapping from the subject eigen space to the template eigen space.

The filter used to implement the standard 2D histogram matching normalizes the grayscale values of a source image (subject FA image in our case) based on the grayscale values of a reference image (atlas FA image in our case). This filter from Insight Toolkit[5] uses a histogram matching technique where the histograms of the two images are matched only at a specified number of quantile values. As a result of this histogram matching, each subject tensor has a corresponding atlas intensity normalized FA value. Let us denote the intensity normalized FA value for the location (x, y, z) as $FANormValue_{x,y,z}$. In our algorithm, after determining the matched iso-MD plane in the atlas space for each subject tensor, we determine the FA values of all the $(\lambda_1, \lambda_2, \lambda_3)$s on this plane based on the equation 1. The $(\lambda_1, \lambda_2, \lambda_3)$s with the most similar FA value to the tensor's intensity normalized FA value $FANormValue_{x,y,z}$ are selected.

$$argmin(FA_i - FANormValue_{x,y,z}) \qquad (4)$$

Substituting equation 1 in the above equation and computing the arg minimum leads to a set of points on the plane. These set of points represented as $(\lambda_{1i,MD,FA}, \lambda_{2i,MD,FA}, \lambda_{3i,MD,FA})$ ($'i'$ indicating the points on the selected iso-MD plane and $'MD'$ and $'FA'$ represent that these points satisfy the condition of closest MD and FA) form an ellipse on the iso-MD plane (Fig. 2). The final step in our method is to determine the point p_{min} from these set of points that satisfies the condition $(\lambda_1 > \lambda_2 > \lambda_3)$ and has the minimum Euclidean distance to the original tensor.

$$p_{min} = argmin((\lambda_{1x,y,z} - \lambda_{1i,MD,FA})^2 +$$
$$(\lambda_{2x,y,z} - \lambda_{2i,MD,FA})^2 + (\lambda_{3x,y,z} - \lambda_{3i,MD,FA})^2)^{0.5} \qquad (5)$$

This minimum Euclidean distance ensures that the normalized tensor has the most similar shape to the original tensor. Hence, this algorithm computes the
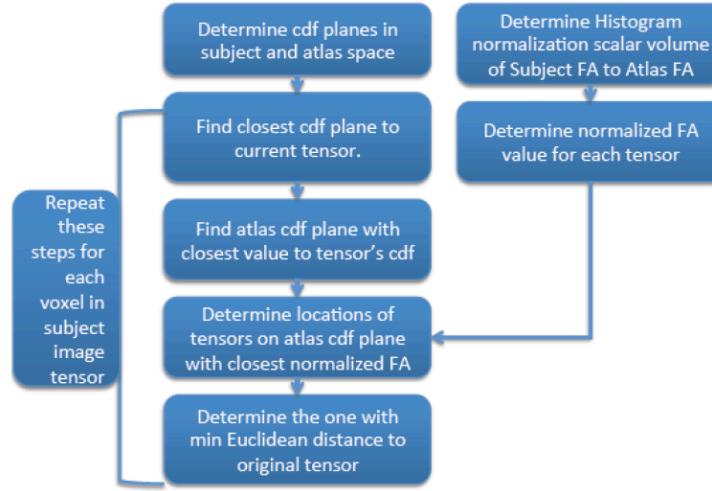
---

[5] www.itk.org

Fig. 3. Block diagram showing all the steps in the normalization algorithm.

normalized tensor with the most similar tensor shape that satisfies the conditions of same cdf and closest normalized FA values. The normalized DTI volume is determined by computing the normalized tensor for each tensor of the subject based on the above steps. For clarity, the block diagram Fig. 3 illustrates all the steps.

3 Experiments

Subjects: The tensor normalization method is tested on Krabbe subjects in the age 10 days to 2 years. These subjects are registered to a neonate atlas (built from 377 age-matched neonate controls) and a 1-2 year atlas (from 283 controls age 1 to 2 year). Both atlases are built using a scalar, unbiased diffeomorphic atlas building method based on a nonlinear high-dimensional fluid deformation method [3]. Details of image acquisition of the controls and Krabbe can be found in [10].

    Setup: Four Krabbe neonates are registered to a neonate atlas using the DTITK algorithm with and without the proposed normalization method. To test the robustness of the normalization wherein there are large anatomical variations between the subject and the atlas, we registered the same four neonates to a 1-2 year atlas (as there are considerable differences from a neonate to a 1-2 year brain). Three additional 1 to 2 year old Krabbe subjects are registered to the 1-2year atlas using the DTITK algorithm. An affine registration is implemented as a preprocessing step prior to DTITK registration. For all the Krabbe subjects, the DTI volumes are normalized using our proposed method and the DTITK deformation field for mapping the normalized subjects to the atlas is determined.

The field is applied to the original (not normalized) DTI and the results are compared.

Tract-based Analysis: In this paper, we prove the performance of the method for atlas based registration methods. Since this is an application based methodology, we focus our evaluation on FA profiles of tract based analysis. The clinicians use the statistics of the FA profiles for their Krabbe subject evaluation. We evaluate the registration with and without normalization via fiber tractography based FA profiles [2] for four fiber tracts - corticospinal internal capsule tracts (left and right), genu and splenium. These tracts have been previously manually extracted from the different atlases. The FA profiles represent the average FA values across the individual streamlines along the tract[2]. Since the tracts under consideration are the prominent high intensity tracts, a higher FA profile indicates a better registration. The comparison is performed between the FA profiles of the four tracts obtained from: 1. Registration of the original DTI to the atlas using DTITK algorithm and obtaining the registered DTI volume in the same space as the atlas. The fiber tracts are extracted from the registered DTI volumes using the previously defined atlas tracts and the transformation field. Using a prior definition of a tract origin plane, which defines a curvilinear re-parameterization of the tracts, corresponding average tract property FA profiles are extracted from each individual fiber tract. 2. The original DTI is normalized using the proposed method. The normalized DTI is registered to the atlas and the deformation field is determined. This deformation field is applied to the original DTI to obtain the atlas registered DTI volume. The fiber tracts are extracted in the similar method as above. 3. A region of interest (ROI) in the tract that is under study is defined by a trained expert for the original DTI of each subject. The FA volume is used as a reference volume to trace the ROI. From the ROI, the fiber tracts are seeded using the tool Slicer3 [6]. The fiber tracts are cleaned to remove crossing fibers and the FA profiles are determined of these tracts using an in-house tool called FiberViewer [7].

Evaluation: The FA profiles from manual tractography ($MeanFA_{mt}$) are considered as the ground truth and compared to the FA profiles of the fiber tracts extracted from the registered original and normalized DTI ($MeanFA_{orig/norm}$). The mean absolute point-wise difference (MAD) normalized by the mean FA of the ground truth is used as the evaluation error metric:

$$E = \frac{MeanFA_{orig/norm} - MeanFA_{mt}}{MeanFA_{mt}} \tag{6}$$

4 Results and Discussions

For the four fiber tracts, the tensor normalization resulted in FA profiles with higher values as compared to the profiles without normalization. In Table 1, we show the percentage error in registration of the major fiber tracts with and without normalization. Compared to the ground truth an average percentage decrease

---

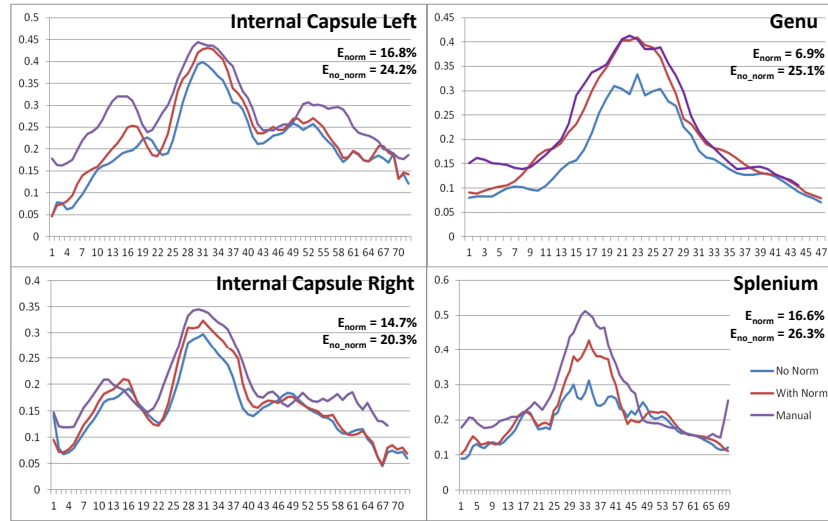[6] www.slicer.org

[7] www.na-mic.org

Fig. 4. Comparison of FA profiles for the four tracts. (x-axis:FA values; y-axis: points along the fiber tracts) For each tract - manual (highest FA), with normalization (middle) and without normalization (lowest FA).

in error of 5 to 10% is observed. For example, for the Genu tract (Neonate3), normalization resulted in a 7% error as compared to 25% error without normalization i.e. an improvement in average FA values from 0.32 to 0.4 (18% improvement). The challenge of registration of Krabbe cases to a normal atlas has been discussed earlier, and a 2 to 18% improvement is substantial. Even in cases of poor registration (eg. left internal capsule Neonate1 mapped in 1-2 year atlas), the normalization improves the registration considerably (11%). The selected tracts are the tracts with the highest FA intensities and thus higher FA values indicate better mapping of the subject into the atlas template i.e. better registration. We observe a higher improvement in registration in the corpus collosum tracts compared to the cortico-spinal tracts. This is likely due to a higher reduction in registration errors that are normally seen in the central bends of the genu and splenium tracts without normalization (see splenium tract in Fig. 4. It is important to note that manual tractography, though performed to the best of our ability by a trained expert, is akin to manual segmentation and is subject to variability. Due to this factor, point-wise comparison and higher variability towards the ends of the tracts, the % error values in Table 1 appear high. Important to this evaluation is the percentage decrease in error rather than the absolute % error.

In most cases, the shape of the FA profile with normalization appears similar to the profile without normalization but with higher values. But in certain cases (splenium profile of Fig. 4), the shape of the FA profile from normalization appears more similar to the ground truth, again indicating an improvement in registration along the entire tract. This method can be easily introduced as

Table 1. Table showing the $E\%$ for 11 cases (7 subjects) and average % error reduction.

In Neonate Atlas	Neonate1		Neonate2		Neonate3		Neonate4	
	No Norm	With Norm	No Norm	With Norm	No Norm	With Norm	No Norm	With Norm
CSIC_left	22.0%	19.5%	25.7%	22.8%	24.1%	20.0%	24.2%	16.8%
CSIC_right	20.3%	14.7%	20.6%	19.0%	21.3%	17.0%	18.1%	11.2%
Genu	22.8%	15.7%	20.6%	15.6%	25.1%	6.9%	38.9%	23.2%
Splenium	26.3%	16.6%	22.6%	21.1%	30.2%	12.1%	38.1%	28.2%

In 1-2year Atlas	Neonate1		Neonate2		Neonate3		Neonate4	
	No Norm	With Norm	No Norm	With Norm	No Norm	With Norm	No Norm	With Norm
CSIC_left	43.6%	32.9%	51.4%	36.4%	25.1%	18.3%	26.2%	18.8%
CSIC_right	35.0%	25.7%	27.5%	18.1%	20.5%	10.9%	34.7%	30.4%
Genu	12.7%	0.6%	13.7%	4.8%	6.6%	2.7%	15.0%	9.7%
Splenium	22.8%	11.5%	27.1%	25.3%	13.3%	8.9%	22.8%	11.8%

In 1-2 year Atlas	1-2year1		1-2year2		1-2year3		Average % reduction in error for 11 cases
	No Norm	With Norm	No Norm	With Norm	No Norm	With Norm	
CSIC_left	24.9%	20.8%	34.0%	22.1%	36.8%	33.7%	5.99%
CSIC_right	28.7%	25.7%	37.4%	34.8%	34.5%	31.6%	5.42%
Genu	14.3%	9.2%	19.7%	14.5%	21.7%	11.0%	9.33%
Splenium	11.0%	6.1%	21.4%	9.1%	25.2%	16.8%	8.47%

a pre-processing step in most analysis pipelines. On a typical workstation, the normalization takes less than 5 minutes. The code is open source and the binaries can be downloaded as a part of the "dtiprocess" package [8].

5 Conclusions

Based on the evaluation criteria, the proposed tensor normalization method considerably improves the registration of the subjects into the atlas template. Even for white matter demylinating diseases like Krabbe, where registration is a very crucial step for analysis, this method gives a significant improvement in the registration accuracy. This method can be very easily introduced as a pre-processing step prior to registration in any analysis pipeline. The normalized DTI

---

[8] www.nitrc.com

is only used for generating the registration diffeomorphic field, and this generated field is applied to the original DTI and hence no properties of the original DTI are altered in this pre-processing step. Our future work will be focused on testing this method on other tensor registration methods like MedINRIA and also on atlas building methods.

6 Acknowledgements

References

1. Escolar, M., Poe, M., Smith, J., Gilmore, J., Kurtzberg, J., Lin, W., Styner, M.: Diffusion tensor imaging detects abnormalities in the corticospinal tracts of neonates with infantile krabbe disease. American Journal of Neuroradiology **30**(5) (May 2009) 1017–1021

2. Goodlett, C.B., Fletcher, P.T., Gilmore, J.H., Gerig, G.: Group analysis of dti fiber tract statistics with application to neurodevelopment. NeuroImage **45**(1, Supplement 1) (2009) S133 – S142

3. Joshi, S., Davis, B., Jomier, M., Gerig, G.: Unbiased diffeomorphic atlas construction for computational anatomy. NeuroImage **23, Supplement 1**(0) (2004) S151 – S160

4. Yap, P.T., Wu, G., Zhu, H., Lin, W., Shen, D.: F-timer: Fast tensor image morphing for elastic registration. Medical Imaging, IEEE Transactions on **29**(5) (may 2010) 1192 –1203

5. Zhang, H., Yushkevich, P.A., Alexander, D.C., Gee, J.C.: Deformable registration of diffusion tensor mr images with explicit orientation optimization. Medical Image Analysis **10**(5) (2006) 764 – 785

6. Wang, Y., Gupta, A., Liu, Z., Zhang, H., Escolar, M.L., Gilmore, J.H., Gouttard, S., Fillard, P., Maltbie, E., Gerig, G., Styner, M.: Dti registration in atlas based fiber analysis of infantile krabbe disease. NeuroImage **55**(4) (2011) 1577 – 1586

7. Verma, R., Davatzikos, C.: Matching of diffusion tensor images using gabor features. In: Biomedical Imaging: Nano to Macro, 2004. IEEE International Symposium on. (april 2004) 396 – 399 Vol. 1

8. Salas-Gonzalez, D., Estrada, J., Gorriz, J., Ramirez, J., Segovia, F., Chaves, R., Lopez, M., Illan, I., Padilla, P.: Improving the convergence rate in affine registration of pet brain images using histogram matching. In: Nuclear Science Symposium Conference Record (NSS/MIC), 2010 IEEE. (30 2010-nov. 6 2010) 3599 –3601

9. Han, J.H., Yang, S., Lee, B.U.: A novel 3-d color histogram equalization method with uniform 1-d gray scale histogram. Image Processing, IEEE Transactions on **20**(2) (feb. 2011) 506 –512

10. Gilmore, J.H., Zhai, G., Wilber, K., Smith, J.K., Lin, W., Gerig, G.: 3 tesla magnetic resonance imaging of the brain in newborns. Psychiatry Research: Neuroimaging **132**(1) (2004) 81 – 85